

Identification of Pathogenesis and Prognoses of Relapse in Myeloma by Bioinformatic Method

Haoshu Zhong

Southwest Medical University

Yang Liu

Affiliated Hospital of Southwest Medical University

Jialin Duan

Southwest Medical University

Xiaomin Chen

Affiliated Hospital of Southwest Medical University

Hao Xiong

Affiliated Hospital of Southwest Medical University

Kunyu Liao

Southwest Medical University

Chunlan Huang (✉ huangchunlan@swmu.edu.cn)

Affiliated Hospital of Southwest Medical University

Research Article

Keywords: Multiple myeloma, Bioinformatics analysis, Prognostic model, drug resistance, tumor metastasis

Posted Date: December 1st, 2021

DOI: <https://doi.org/10.21203/rs.3.rs-1100874/v1>

License:   This work is licensed under a Creative Commons Attribution 4.0 International License.

[Read Full License](#)

Abstract

Background: Multiple myeloma (MM), the second most hematological malignancy, the molecular mechanism and pathogenesis of the relapse of MM is poorly understood. This study aimed to identify novel prognostic model for MM and explore potential mechanism of relapse.

Methods: Gene expression data, clinical data (GSE24080) and HTseq-Counts files were downloaded from Gene Expression Omnibus (GEO) and TCGA database. Co-expression modules of genes were built by Weighted Correlation Network Analysis (WGCNA). KEGG and GO enrichment analysis were performed in each module. TATFs (tumor-associated transcription factors) were retrieved from the Cistrome. Twenty-two immune cell compositions was calculated by CIBERSORT algorithm. Univariate and multivariate Cox regression were performed and a predictive model by prognostic genes was constructed, the predictive power of the model was evaluated by Kaplan–Meier curve and time-dependent receiver operating characteristic (ROC) curves.

Results: A total of 940 DEGs were identified, and in WGCNA analysis, yellow, brown and sky-blue modules were most associated with clinic traits. The yellow module related with the cell cycle and the brown and sky-blue modules correlated with cytokine and its receptors, where the M2 macrophage fraction is positively correlated with CCL18, CCL2, CCL8, CXCL12 and CCL23 were positively correlated with plasma cells by CIBERSORT analysis. Prognostic genes were identified and two genes (TPX2, PRAM1) were finally identified to construct a risk model for predicting EFS.

Introduction

Multiple myeloma (MM, plasma cell myeloma) is a malignant hematologic disease characterized by the clonal proliferation of malignant plasma cells. The treatment of MM has changed dramatically in recent years, with the use of proteasome inhibitors, immunomodulatory agents, and autologous hematopoietic stem cell transplantation in MM patients combined with standard chemotherapy, the survival of MM patients has been significantly prolonged, but all patients will eventually relapse and often demonstrate multiple drug resistance [1]. Besides, new technologies and methods such as CNV Radar to define a riskscore of MM for informing clinical and therapeutic decisions [2]. Weighted gene co-expression network (WGCNA) are also a systems biology approach for describing the correlation patterns among genes across samples and can be used to find clusters (modules) of highly correlated genes, summarize these clusters using the module eigengene or an intramodular hub gene, correlate intermodule and external sample traits (using eigengene network methodology), and calculate module membership metrics [3]. The correlation networks facilitate network based gene screening methods that can be used to identify candidate biomarkers or therapeutic targets. It has been widely utilized in many malignant diseases and non-malignant diseases. In the present study, we aimed to use WGCNA approach to identify co-expression networks with MM recurrence and identify novel prognostic models, and to elucidate the molecular mechanism and pathogenesis in the relapse of myeloma to understand the function and interrelationships among abnormally expressed genes.

Materials And Methods

Data preparation

The gene expression and clinical information data of GSE24080[4] were downloaded from the gene expression omnibus (GEO) website (<http://www.ncbi.nlm.nih.gov/geo/>). A total of 559 cases (including training and validation sets) were performed based on the GPL96 platform ([HG-U133A]Affymetrix human genome U133A array). There were 553 cases were examined for event-free survival (disease relapse or progression) and additional clinical information was selected to identify prognostic genes and to construct a prognostic model in GSE24080. HTseq-Counts data was obtained from The Cancer Genome Atlas (TCGA) website (<https://portal.gdc.cancer.gov>). Total 47 patients(94 samples) at two different time point(primary and recurrence) were used to identify DEGs. Raw counts were transformed into TPM for WGCNA analysis and correlation between genes.

Screening of differentially expressed genes (DEGs)

The differentially expressed genes(DEGs) between primary and recurrent myeloid-derived cancers were screened from HTseq-Counts of 47 patients at 2 different critical times(primary and relapsed). DEseq2[5] package was used to identify DEGs with R-4.1.1, and the threshold value was $|\log_2\text{foldchange}| > 1.0$ and $\text{adj.P.Val} < 0.05$.

GO term and KEGG pathway enrichment analysis

To better explore the biological function and signal pathway of DEGs in module genes, we performed Gene Ontology (GO) and Kyoto Encyclopedia of Genes and Genomes (KEGG) pathway enrichment analysis using the R package clustering profiler[6] and used a p.value < 0.05 as the cutoff value for clustering.

Co-expression network analysis

The co-expression network was constructed by the R package WGCNA[7] to explore the co-expression of genes (using all protein-coding genes) and clustered into different modules. The PickSoft threshold function of WGCNA was used to calculate the soft threshold power β value, mean connection k and R^2 . The soft power was set to 7 and the scale-free networks were validated by a power-law distribution. Then, we constructed co-expression modules and used gene significance (GS) and module membership (MM) metrics to identify potential modules with both high trait significance and module membership which are significantly related to clinic traits (relapse). Module membership was the correlation between gene expression profiles and module eigengene. GS was the absolute value of correlation between gene expression and module traits.

Identification of prognostic key genes and construction of the prognostic model

Key genes were identified from both hub genes and the DEGs. All patients were randomized into two groups (289 cases in the training set and 264 cases in the test set) and univariate and multivariate Cox regression analyses were used to investigate the correlation between EFS and the expression level of key genes with package survival[8]. P-value <0.001 was considered as a significant difference for univariate analysis. Key genes with P < 0.001 based on the univariate analysis were further included in multivariate Cox regression analysis. After three validation sets. Finally, a prognostic riskscore model of MM patients was established based on linear combination of regression coefficient multiplied by expression level from multivariate Cox regression models. The predictive accuracy of our model was evaluated by classifying patients into low- and high-risk groups based on the optimal cut-off value Kaplan–Meier (K–M) survival curves, time-dependent ROC curve analyses and area under the curve (AUC). Also the prognostic models were validated in the validation set and whole set by K–M curves, ROC curve analyses, and AUC[9].

Identification of independent prognostic parameters of MM

To identify the independence of our model, we enrolled additional clinical information to verify whether our model was independent by multivariate Cox regression analyses of 484 patients with clinic data (missing values were discarded). In addition to risks core, PROT (treatment protocol (TT2 or TT3)), ISOTYPE (IgA, IgD, IgG), B2M (Beta-2 microglobulin, mg/L), LDH (Lactate dehydrogenase, U/L), MRI (number of magnetic resonance imaging-defined focal lesions (skull, spine, pelvis)), BMPC (bone marrow biopsy plasma cells (%)), HGB (Haemoglobin, g/dl) and RACE (Race (white or other)) were included in the analyses. It shows that the risk score and isotype LDH/B2M of our model have prognostic value. They are independent of EFS in myeloma patients.

Tumor-associated transcription factors (TATFs) expression relationship with co-expressed genes

A total of 318 TATFs were retrieved from the Cistrome (<http://cistrome.org/>)[10], and TATFs that were both DEGs and module genes were considered as key regulatory transcription factors. The correlation coefficient value of TATFs' expression levels with the remaining genes in each module were then calculated. For visualization, we used $p\text{-value} \leq 0.05$, correlation coefficient ≥ 0.5 and $p\text{-value} \leq 0.0001$ in the yellow module, correlation coefficient ≥ 0.8 in the brown module, and no TATFs in the sky blue to construct the TATFs-gene regulatory network. And the software cytoscape was used to visualize the regulatory network.

Cell-Type Identification by Estimating Relative Subsets of RNA Transcripts (CIBERSORT)

By the CIBERSORT algorithm (<http://cibersort.stanford.edu/>), twenty-two immune cell compositions of bone marrow specimens were characterized based on the mRNA expression profiling of the GSE24080

data set .The perm was set at 1000. Specimens with $p < 0.05$ were used for analyses. These immune cells including B cells naive, B cells memory, plasma cells, CD8 T cells, T cells CD4, naive T cells, CD4 memory resting, T cells CD4 memory activated, T cells follicular helper, T cells regulatory (Tregs), T cells gamma delta, NK cells resting, activated NK cells, monocytes, macrophages M0, macrophages M1, macrophages M2, dendritic cells resting, dendritic cells activated, mast cells resting, mast cells activated, eosinophils, and neutrophils. Correlation analyses were performed for different immune cells in each sample with interested chemokine. Differences in 22 immune cells scores in multiple myeloma bone marrow specimens were assessed by the Mann-Whitney U-test. Correlations of 17 kinds of cytokine expression with immune cell fractions in bone marrow samples were examined using Pearson correlation analysis.

Results

Identification of DEGs in MM and the enrichment of DEGs

The DEGs screened from TCGA include 20 down-regulated genes and 920 up-regulated genes (Fig. 1A). To clarify the differentially expressed genes, we formed a heat map using the top 400 genes to (Fig. 1B). Then KEGG and GO analyses were further performed to find out the general glimpse functions of differentially expressed genes. By KEGG analysis, DEGs were mainly and significantly enriched in cytokine receptor interaction, hematopoietic cell lineage, cell adhesion molecules, chemokine signaling pathway and NF- κ B osteoclast differentiation, which were important pathways in the pathogenesis of myeloma. The next GO enrichment showed significant immunoreceptor activity, CXCR chemokine receptor binding, myeloid leukocyte migration and chemotaxis, and neutrophil enrichment.

Co-expression Analysis and Identification of Scale-free Network

Weighted correlation network analysis (WGCNA) was conducted to investigate the association between primary and recurrence of myeloma. To ensure that the scale-free network 7 was set to the optimal soft threshold power to ensure proper R^2 obedience to the power distribution and sufficient average connectivity for networks construction. The 400 genes were sampled and clustered to construct a visual topological matrix network (Fig. 2F).

After picking a soft threshold power, we clustered the gene expression into the dynamic shear trees, and trees with similarities above 0.75 were considered highly similar, so they were merged into one tree (Fig. 3A). Next, we included group (primary and recurrent) features in the analysis and calculated to distinguish modules highly associated with myeloma recurrence, then described the correlation coefficients and p-values between GS and MM in the three modules, which were found to be highly correlated, and finally selected genes in the brown sky blue and yellow modules for further study.

Enrichment analysis In each module

In the brown module,CCR chemokine receptor binding and chemokine activity were enriched,and a total of 19 different types of cytokine or its receptors were up-regulated in recurrent myeloma.(supplementary table3)297 Genes were mainly and significantly enriched in Nicotinamide adenine dinucleotide and Cytokine-cytokine receptor interaction in the sky blue module.In the yellow module yellow module there are 882 genes with GO terms mostly related to "Cell cycle".

Immune cells infiltration cytokine relationship and TATFs-gene regulatory network

3 TATFs (CEBPA,ELF5 and CENPA) were upregulated. CEBPA and ELF5 were tumor associated transcription factors in the brown module of the TATFs gene regulatory network (Fig. 5A). Expression of CEBPA and ELF5 was highly positively correlated with chemokine gene expression levels(such as CC13,CCL8,CCL23, CCL16, CCL 24) (supplementary table 2),suggesting that CEBPA may play a central role in the skewed chemokine/chemokine receptor axis. CENPA containing aberrantly regulated genes in the yellow module(Fig. 5B). The wider the borderline,the stronger the correlation coefficient between genes.Each gene played a role in the network and,in addition, we functionally classified the genes according to their up-regulation that may lead to tumor cell proliferation,anti-apoptosis and maintenance(Table 1). Genes expression of 17 differentially up-regulated cytokine and receptors from both brown and sky blue modules were selected to calculate the cor relationship with immune cell infiltration,showing that CCL18,CCL2,CCL8,CXCL12 were related to M2 Macrophages infiltration and CCL23 with plasma cells(Fig. 6).

Table 1

Function of dysregulatory genes in yellow module

Function involved	dysregulatory genes					
Ubiquitin-proteasome pathway	CCNF ¹²	DLGAP5 ¹³	AURKB ¹⁴	CDC20 ¹⁵		
Chromatin stability	CDCA5 ¹⁶	CENPA ¹⁷				
DNA replication	MCM10 ¹⁸	CDT1 ¹⁹	E2F2 ²⁰			
Mitosis	AURKB ²¹	DLGAP5 ²²	CDT1 ¹⁹	BIRC5 ²³	SKA1 ²⁴	KIF20A ²⁵
Component of Chromosome passenger complex	AURKB ²⁶	BIRC5 ²³				
Regulator of resting B- and T-lymphocytes	AURKB ²¹					
Cytokinesis	DIAPH3 ²⁷	BIRC5 ²³	KIF20A ²⁸	CENPA ²⁹	AURKB ²¹	
Transcription activator or repressor	E2F2 ²⁰	E2F8 ³⁰	CCNF ¹²			
P53 signal pathway repressor	E2F8 ³⁰	AURKB ³¹	DLGAP5 ¹³			

Identification of prognostic genes from both DEGs and hub genes

Hub genes were screened by a filtering condition of GS(gene significance) higher than 0.2 and MM (module- membership) higher than 0.8. Next, previously identified DEGs were compared with hub genes (blue 93, brown 297 and yellow 154, Fig. 7) and the overlap part was identified as pivotal prognosis genes for further study. A total of 396 prognostic genes were selected for prognosis analysis.

Independence test of two-gene based signature and other clinic parameters

A two-gene prognostic model (risk score) revealed the independent prognostic capacity of MM patients in relation to other clinical parameters. It showed that our risk scoring model (HR=1.70514, P<0.001) and isotype LDH/B2M of our model have prognostic value. They are independent determinants of EFS in myeloma patients.

Identification prognosis of EFS with key genes and construction of two-gene prognostic signature

Finally, univariate and multivariate COX proportional regression analyses were performed using the potential key genes identified both from hub genes in each module and the above (Fig. 7) mentioned DEGs associated with EFS in MM patients. A total of 396 key genes were identified, and after screening in the training set, validation set and whole set, two genes (TPX2, PRAM1) with constant and independent prognosis value were eventually selected to construct a prognostic model (Fig. 9A. Risk score = (1.48739 expression level of TPX2) + (0.62980 expression level of PRAM1) to assess the prognostic value of these key genes in MM patients. Next, we calculated the optimal cut-off value of two-gene expression as risk score and divided patients in the training set (n = 289) into high-risk group and low-risk group. The Kaplan–Meier (K-M) curves showed that the high-risk group had a worse prognosis than the low-risk group (P < 0.0001), and the gene risks core heatmap was illustrated above (Fig. 9A-C). As the increase of risk score value, the expression level of TPX2 increased but PRAM1 decreased, indicating that TPX2 was a risk factor for the recurrence of MM, while PRAM1 may play a protective role. The AUCs of time-dependent ROC curves were calculated to assess the prognostic capacity of the two-gene signature. AUCs of risk score for the 2-, 3-, and 4-year EFS time training sets were 0.717, 0.643 and 0.624. Respectively, to verify the predictive value of the two-gene signature, we used the internal test set (n = 264) and whole set (n = 553) to appraise the reliability of the training set. The K–M survival curves and AUCs for the validating set and whole set were consistent with the training set. The AUCs of risk score in validating set at 2-, 3-, and 4-year EFS time were 0.732, 0.722 and 0.674, and the whole set were 0.738, 0.691 and 0.657 respectively.

Discussion

Bone marrow micro environment contains cellular components, extracellular matrix and soluble components that form a heterogeneous networks and play an important role in the occurrence and development of myeloma. And WGCNA is a suitable tool to identify the causes and mechanism of myeloma recurrence by identifying the weighted co-expression relationships among genes and then clustering them into highly synergistic modules. Genes with strong relationships between clinic trait and modules were selected for KEGG and GO enrichment analysis, followed by TATFs-gene regulatory network. We found that three modules play different roles in the relapse of myeloma. As the study progressed, we found 19 kinds of cytokine/cytokine receptors upregulated in relapsed myeloma patients in brown module (Supplementary Table 4), with CC13, CCL8, CCL23, CCL16, CCL24, IL18 thought to be regulated by TATFs (CEBPA and ELF5). CCL18, CCL2, CCL8, CXCL12 were related to infiltration of M2 Macrophages.

CCL18 secreted by M2 macrophages promotes tumor cell migration and invasion in gallbladder cancer [32]. CCL2 promotes macrophages-associated chemoresistance in multiple myeloma [33]. CCL8 promotes postpartum breast cancer by recruiting M2 macrophages [34]. A study showed that inhibition of M2 polarization can overcome myeloma resistance to lenalidomide by reducing CXCL12 expression [35]. However, the relationship between CCL18 and CCL8, M2 macrophages and myeloma recurrence has not been studied yet.

A large number of cytokine such as CXCL-12, IL-6, IL-8 and IL-17 have been elucidated and they construct a pro-inflammatory and permissive environment for the survival of myeloma cells[36]. Some mechanism of myeloma are finely elucidated, but the role of cytokine are still remaining unclear in the relapse of myeloma, and we provide dysregulated cytokine and their relationship with CEBPA and ELF5, suggesting that receptors for chemokine are an important point, as pharmacological inhibitors of individual receptors may have limited efficacy due to the redundancy, as well as a tendency toward compensatory increased expression of other chemokine family members[37]. So it's critical to discover that key gene regulating cytokines and blocking them may simultaneously cause the turnover of a large number of chemokine, thus overcoming drug resistance and allowing cells to promote apoptosis and prevent myeloma cell metastasis. We therefore hypothesize that CEBPA and ELF5 may be the potential target for reversing cytokine.

In the CENPA-based regulatory network, we provide another possible pathogenesis of myeloma recurrence. In the yellow module, high expression of CENPA in relapsed myeloma was positively related to E2F2, suggesting that E2F2 may be associated with poor prognosis, after all, its expression in breast cancer correlated with lower recurrence-free survival[38]. BIRC5/survivin: A multitasking protein with dual roles in promoting cell proliferation and preventing apoptosis. Overexpression of AURKA lead to drug resistance in gastric cancer by up-regulating the gene expression of the anti-apoptotic protein survivin[39].

Furthermore, over-expression of survivin in the presence of anti-myeloma drugs was found to increase the viability of MM cells[40]. SKA1: knockdown of SKA1 shows a significant reduction in proliferation of bladder cancer cells[41]. DIAPH3: Highly expressed DIAPH3 promoted proliferation, non-anchored growth and invasion of pancreatic cancer cells[42]. Genes above are upregulated in yellow module, revealing that CENPA and other genes may play a key role in cell cycle, which lead to myeloma recurrence and promote tumor proliferation and drug resistance. The high level of genes expression in the yellow module has been rarely studied in myeloma, which provide a new direction for our research in myeloma patients.

In sky blue module: BST1 is found in relapsed multiple myeloma patients at a expression foldchange level of 4. BST1 is a analogue of CD38, which has similar functions such as hydrolysis NAD⁺ to adenosin (ADO). BST1 produce adenosine diphosphate ribose (ADPR) which is subsequently converted to AMP and eventually to ADO, causing immunosuppressive functions, and is also growth factor for osteoblasts and osteoclasts. Interestingly BST1/CD157 was undetectable in myeloma cell line, suggesting that upregulated BST1 is a key cause of relapse in patients[43]. The association between BST1 and drug resistance in myeloma cells have not been reported, and the high level of BST1 expression in our study suggests that it may contribute to the survival and immune escape of myeloma cells, leading to the recurrence of the disease.

Two of our screens from the hub genes were used to determine prognosis. TPX2 and PRAM1 showed independent predictive power in predicting EFS in myeloma, and both sets of genes have been rarely reported in myeloma. TPX2 is a spindle assembly factor required for mitotic spindles, and normal

assembly, and its inhibition lead to a significant increase in mitotic index and metaphase myeloma cells. Therefore, it may be feasible to obtain inhibitors from it to suppress myeloma proliferation cells [44]. Furthermore, high levels of TPX2 indicated lower survival rate and promoted cancer cell migration and invasion in Non-Small Cell Lung Cancer [45]. PRAM1 had never been reported in research of myeloma, but the high expression of PRAM1 is a sign for favorable prognosis in the CN-AML [46]. This is consistent with our study that TPX2 is associated with high recurrence rates and PRAM1 gene expression is a protective factor in patients with myeloma.

The present study has several strengths and limitations. Bioinformatic tools have been used in our study to provide a general but comprehensive understanding of the mechanism of myeloma recurrence at the transcriptome level, and we provide some potential area of study worthy of in-depth study to overcome drug resistance and metastasis. A series of pivotal genes and response group pathways were identified to elucidate the molecular mechanisms of myeloma recurrence and to identify potential therapeutic targets. However, this study does not go deep enough and more experiments are needed to validate the function of molecules in the regulatory networks of multiple myeloma patients.

Conclusion

In summary, we have used bio-informatics tools to elucidate possible signaling pathways and co-expressed genes regulatory network that may contribute to relapse in multiple myeloma patients. And a two-gene (TPX2, PRAM1) based prognostic model was identified and constructed, which can be used to predict overall event-free survival (EFS) in MM patients.

Declarations

Ethics approval and consent to participate

Not applicable.

Consent for publication

Not Applicable

Availability of data and material

The datasets analyzed during this study are publicly available in GEO database at <https://www.ncbi.nlm.nih.gov/geo/> and TCGA database at <https://portal.gdc.cancer.gov/>

Competing interests

The author declare that they have no conflict of interest.

Funding

There is no relevant funding for this study.

Authors' contributions

HZ and CH conceived and designed the study, as well as designed the figures and tables. HZ and YL contributed to the statistical analysis, JD, XC, HX, KL, drafted and correcting the manuscript. All authors read and approved the final manuscript.

Acknowledgments

The authors would like to thank the TCGA and GEO databases developed by the National Institutes of Health.

References

1. Pawel Robak, Izabela Drozd, Janusz Szemraj, Tadeusz Robak. Drug resistance in multiple myeloma. *Cancer Treat Rev.* 2018 Nov; 70:199-208.
2. David Soong, Jeran Stratford, Herve Avet-Loiseau, Nizar Bahlis, Faith Davies, Angela Dispenzieri. CNV Radar: an improved method for somatic copy number alteration characterization in oncology. *BMC Bioinformatics.* 2020 Mar 6; 21(1):98.
3. Bin Zhang, Steve Horvath. A general framework for weighted gene co-expression network analysis. *Statistical Applications in Genetics and Molecular Biology.* Stat Appl Genet Mol Biol. 2005; 4: Article 17.
4. Shi L, Campbell G, Jones WD, Campagne F et al. The MicroArray Quality Control (MAQC)-II study of common practices for the development and validation of microarray-based predictive models. *Nat Biotechnol* 2010 Aug; 28(8):827-38.
5. Love, M.I., Huber, W., Anders, S. Moderated estimation of fold change and dispersion for RNA-seq data with DESeq2 *Genome Biology* 15(12):550 (2014)
6. T Wu, E Hu, S Xu, M Chen, P Guo, Z Dai, T Feng, L Zhou, W Tang, L Zhan, X Fu, S Liu, X Bo, and G Yu. clusterProfiler 4.0: A universal enrichment tool for interpreting omics data. *The* 2021, 2(3):100141
7. Peter Langfelder, Steve Horvath. WGCNA: an R package for weighted correlation network analysis. *BMC Bioinformatics.* 2008 Dec 29; 9:559.
8. Terry M. Therneau, Patricia M. Grambsch. *Modeling Survival Data: Extending the Cox.* *Statistics for Biology and Health* (2000). 10.1007/978-1-4757-3294-8.
9. Heagerty PJ, Zheng Y. 2005. Survival model predictive accuracy and ROC curves. *Biometrics.* Biometrics. 2005 Mar; 61(1):92-105.
10. Mei S, Qin Q, Wu Q, Sun H, Zheng R, Zang C, Zhu M, Wu J, Shi X, Taing L, et al. Cistrome data browser: a data portal for ChIP-Seq and chromatin accessibility data in human and mouse. *Nucleic Acids Res.* 2017 Jan 4; 45(D1):D658-D662.
11. Newman AM, Liu CL, Green MR, Gentles AJ, Feng W, Xu Y, et al. Robust enumeration of cell subsets from tissue expression profiles. *Nat Methods.* Nat Methods. 2015 May; 12(5):453-7.

12. Linda Clijsters, Claire Hoencamp, Jorg J A Calis, Antonio Marzio, Shanna M Handgraaf, Maria C Cuitino et al. Cyclin F controls cell cycle transcriptional outputs by directing the degradation of the three activator E2Fs. *Mol Cell*. 2019 Jun 20;74(6):1264-1277.e7.
13. Tzu-Ching Kuo, Pu-Yuan Chang, Shiu-Feng Huang, Chen-Kung Chou, Chuck C-K Chao. Knockdown of HURP inhibits the proliferation of hepatocellular carcinoma cells via downregulation of gankyrin and accumulation of p53. *Biochem Pharmacol*. 2012 Mar 15;83(6):758-68.
14. Wahafu Alafate, Jie Zuo, Zhong Deng, Xiaoye Guo, Wei Wu, Wei Zhang et al. Combined elevation of AURKB and UBE2C predicts severe outcomes and therapy resistance in glioma. *Pathol Res Pract*. 2019 Oct;215(10):152557.
15. Virginia Amador, Sheng Ge, Patricia G Santamaría, Daniele Guardavaccaro, Michele Pagano. APC/C(Cdc20) controls the ubiquitin-mediated degradation of p21 in prometaphase. *Mol Cell*. 2007 Aug 3;27(3):462-73.
16. Julia Schmitz, Erwan Watrin, Péter Lénárt, Karl Mechtler, Jan-Michael Peters. Sororin is required for stable binding of cohesin to chromatin and for sister chromatid cohesion in interphase. *Curr Biol*. 2007 Apr 3;17(7):630-6.
17. Megan A Mahlke, Yael Nechemia-Arbely. Guarding the Genome: CENP-A-Chromatin in Health and Cancer. *Genes (Basel)*. 2020 Jul 16;11(7):810.
18. Marko Lõoke, Michael F Maloney, Stephen P Bell. Mcm10 regulates DNA replication elongation by stimulating the CMG replicative helicase. *Genes Dev*. 2017 Feb 1;31(3):291-305.
19. Hui Zhang. Regulation of DNA Replication Licensing and Re-Replication by Cdt1.
20. E2F2 represses cell cycle regulators to maintain quiescence. *Int J Mol Sci*. 2021 May 14;22(10):5195.
21. Alberto Frangini, Marcela Sjöberg, Monica Roman-Trufero, Gopuraja Dharmalingam, Vanja Haberle, Till Bartke. The aurora B kinase and the polycomb protein ring1B combine to regulate active promoters in quiescent lymphocytes. *Mol Cell*. 2013 Sep 12;51(5):647-61.
22. Ann-Ping Tsou, Chu-Wen Yang, Chi-Ying F Huang, Ricky Chang-Tze Yu, Yuan-Chii G Lee, Cha-Wei Chang et al. Identification of a novel cell cycle regulated gene, HURP, overexpressed in human hepatocellular carcinoma. *Oncogene*. 2003 Jan 16;22(2):298-307.
23. Queenie P Vong, Kan Cao, Hoi Y Li, Pablo A Iglesias, Yixian Zheng. Chromosome Alignment and Segregation Regulated by Ubiquitination of Survivin. *Science*. 2005 Dec 2;310(5753):1499-504.
24. Amit Rahi, Manas Chakraborty, Kristen Vosberg, Dileep Varma. Kinetochore-microtubule coupling mechanisms mediated by the Ska1 complex and Cdt1. *Essays Biochem*. 2020 Sep 4;64(2):337-347.
25. Wen-Da Wu, Kai-Wei Yu, Ning Zhong, Yu Xiao, Zhen-Yu She. Roles and mechanisms of Kinesin-6 KIF20A in spindle organization during cell division. *Eur J Cell Biol*. 2019 Jun;98(2-4):74-80.
26. Mar Carmena, Michael Wheelock, Hironori Funabiki, William C Earnshaw. The Chromosomal Passenger Complex (CPC): From Easy Rider to the Godfather of Mitosis. *Nat Rev Mol Cell Biol*. 2012 Dec;13(12):789-803.

27. Hiroki Kazama, Shu-Ichiro Kashiwaba, Sayaka Ishii, Keiko Yoshida, Yuta Yatsuo, Takuma Naraoka. Loss of DIAPH3, a Formin Family Protein, Leads to Cytokinetic Failure Only under High Temperature Conditions in Mouse FM3A Cells. *Int J Mol Sci.* 2020 Nov 11;21(22):8493.
28. Rüdiger Neef, Christian Preisinger, Josephine Sutcliffe, Robert Kopajtich, Erich A Nigg, Thomas U Mayer et al. Phosphorylation of mitotic kinesin-like protein 2 by polo-like kinase 1 is required for cytokinesis. *J Cell Biol.* 2003 Sep 1;162(5):863-75.
29. S G Zeitlin, R D Shelby, K F Sullivan. CENP-A is phosphorylated by Aurora B kinase and plays an unexpected role in completion of cytokinesis. *J Cell Biol.* 2001 Dec 24;155(7):1147-57.
30. Jing Li, Cong Ran, Edward Li, Faye Gordon, Grant Comstock, Hasan Siddiqui et al. Synergistic Function of E2F7 and E2F8 is Essential for Cell Survival and Embryonic Development. *Dev Cell.* 2008 Jan;14(1):62-75.
31. Jing Li, Cong Ran, Edward Li, Faye Gordon, Grant Comstock, Hasan Siddiqui et al. Aurora B interacts with NIP-p53, leading to p53 phosphorylation in its DNA-binding domain and subsequent functional suppression. *Dev Cell.* 2008 Jan;14(1):62-75.
32. Zhenyu Zhou, Yaorong Peng, Xiaoying Wu, Shiyu Meng, Wei Yu, Jinghua Zhao. CCL18 secreted from M2 macrophages promotes migration and invasion via the PI3K/Akt pathway in gallbladder cancer. *Cell Oncol (Dordr).* 2019 Feb;42(1):81-92.
33. Ruyi Xu, Yi Li, Haimeng Yan, Enfan Zhang, Xi Huang, Qingxiao Chen. CCL2 promotes macrophage-associated chemoresistance via MCP1P1 dual catalytic activities in multiple myeloma. *Cell Death Dis.* 2019 Oct 14;10(10):781.
34. Elena Farmaki, Vimala Kaza, Ioulia Chatzistamou, Hippokratis Kiaris. CCL8 Promotes Postpartum Breast Cancer by Recruiting M2 Macrophages. *iScience.* 2020 Jun 26;23(6):101217.
35. Haiming Chen, Mingjie Li, Eric Sanchez, Camilia M Soof, Sean Bujarski, Nicole Ng. JAK1/2 pathway inhibition suppresses M2 polarization and overcomes resistance of myeloma to lenalidomide by reducing TRIB1, MUC1, CD44, CXCL12, and CXCR4 expression. *Br J Haematol.* 2020 Jan;188(2):283-294.
36. Jan Korbecki, Klaudyna Kojder, Donata Simińska, Romuald Bohatyrewicz, Izabela Gutowska, Dariusz Chlubek et al. CC Chemokines in a Tumor: A Review of Pro-Cancer and Anti-Cancer Properties of the Ligands of Receptors CCR1, CCR2, CCR3, and CCR4. *Int J Mol Sci.* 2020 Nov 9;21(21):8412.
37. Salvatore J Coniglio. Role of Tumor-Derived Chemokines in Osteolytic Bone Metastasis. *Front Endocrinol (Lausanne).* 2018 Jun 7;9:313.
38. Cheng-Cao Sun, Shu-Jun Li, Wei Hu, Jian Zhang, Qun Zhou, Cong Liu, Lin-Lin Li et al. Comprehensive Analysis of the Expression and Prognosis for E2Fs in Human Breast Cancer. *Mol Ther.* 2019 Jun 5;27(6):1153-1165.
39. M Kamran, Z-J Long, D Xu, S-S Lv, B Liu, C-L Wang et al. Aurora kinase A regulates Survivin stability through targeting FBXL7 in gastric cancer drug resistance and prognosis. *Oncogenesis.* 2017 Feb 20;6(2):e298.

40. Jahangir Abdi, Nasrin Rastgoo, Yan Chen, Guo An Chen, Hong Chang et al. Ectopic expression of BIRC5-targeting miR-101-3p overcomes bone marrow stroma-mediated drug resistance in multiple myeloma cells. *BMC Cancer*. 2019 Oct 21;19(1):975.
41. Feng Tian, Xiaoxiao Xing, Feng Xu, Wen Cheng, Zhengyu Zhang, Jianping Gao et al. Downregulation of SKA1 Gene Expression Inhibits Cell Growth in Human Bladder Cancer. *Cancer Biother Radiopharm*. 2015 Sep;30(7):271-7.
42. Yefei Rong, Jie Gao, Tiantao Kuang, Jianlin Chen, Jian-Ang Li, Yufeng Huang et al. DIAPH3 promotes pancreatic cancer progression by activating selenoprotein TrxR1-mediated antioxidant effects. *J Cell Mol Med*. 2021 Feb;25(4):2163-2175.
43. Valeria Quarona, Valentina Ferri, Antonella Chillemi, Marina Bolzoni, Cristina Mancini, Gianluca Zaccarello et al. Unraveling the contribution of ectoenzymes to myeloma life and survival in the bone marrow niche. *Ann N Y Acad Sci*. 2015 Jan;1335:10-22.
44. Christopher A Maxwell, Jonathan J Keats, Andrew R Belch, Linda M Pilarski, Tony Reiman. Receptor for Hyaluronan-Mediated Motility Correlates with Centrosome Abnormalities in Multiple Myeloma and Maintains Mitotic Integrity. *Cancer Res*. 2005 Feb 1;65(3):850-60.
45. Wahafu Alafate, Jie Zuo, Zhong Deng, Xiaoye Guo, Wei Wu, Wei Zhang et al. Combined elevation of AURKB and UBE2C predicts severe outcomes and therapy resistance in glioma. *Pathol Res Pract*. 2019 Oct;215(10):152557.
46. Na Lv, Kun Qian, Jing Liu, Li-Li Wang, Yong-Hui Li, Li Yu. Investigation of PRAM1 Expression Features and Their Clinical Significance in AML via Gene Expression Microarray Database. *Zhongguo Shi Yan Xue Ye Xue Za Zhi*. 2018 Apr;26(2):368-374.

Figures

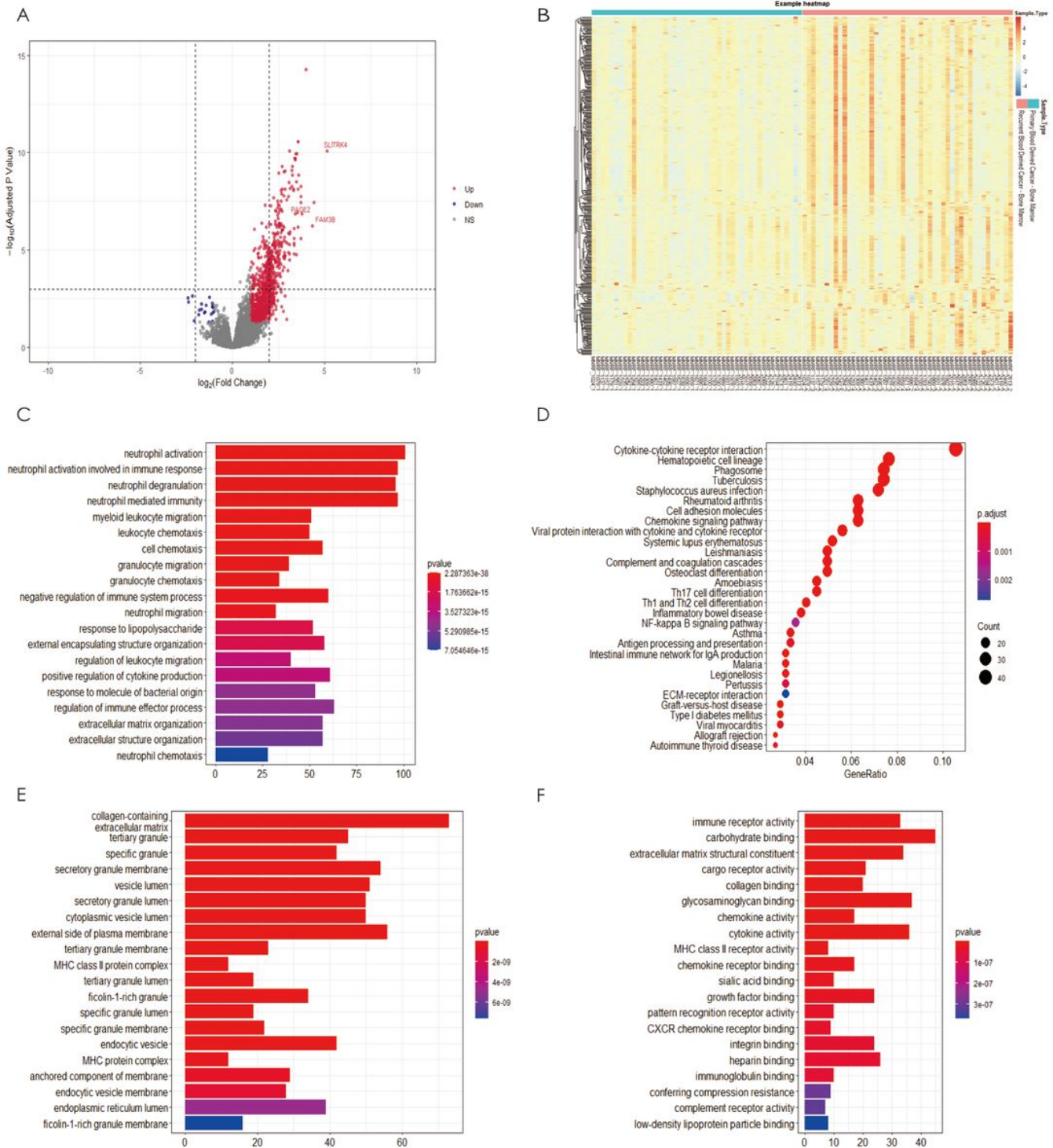


Figure 1

Differential expression of DEGs in primary and relapsed myeloid-derived cancers. Volcano map (A) and heatmap of the DEGs (top400 genes)(B)of DEGs between the two group. In the enrichment analysis of DEGs, C, E-F show the top 20 GO terms, while D shows the top 30 KEGG pathways.

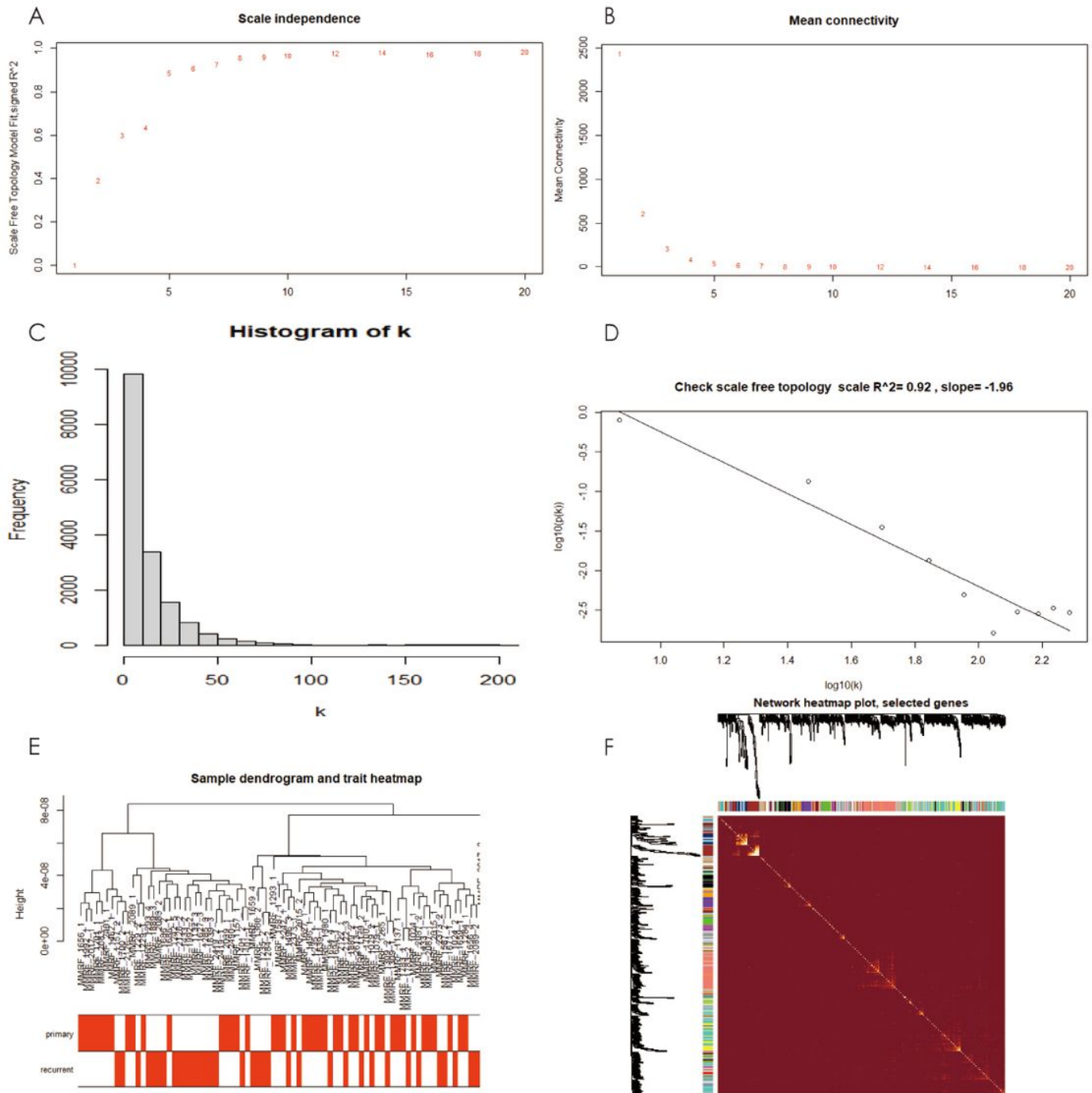


Figure 2

Determination of soft threshold power. (A) Analysis of the scale-free fitting indices for various soft threshold powers. (B) Average connectivity analysis of various soft threshold powers. Histogram showing connectivity distribution. (C) and examination of scale-free topology (D) when $\beta = 7$. (E) Sample cluster map and sample feature heat map of whole genes. (F) Heat map of topological matrix of 400 genes

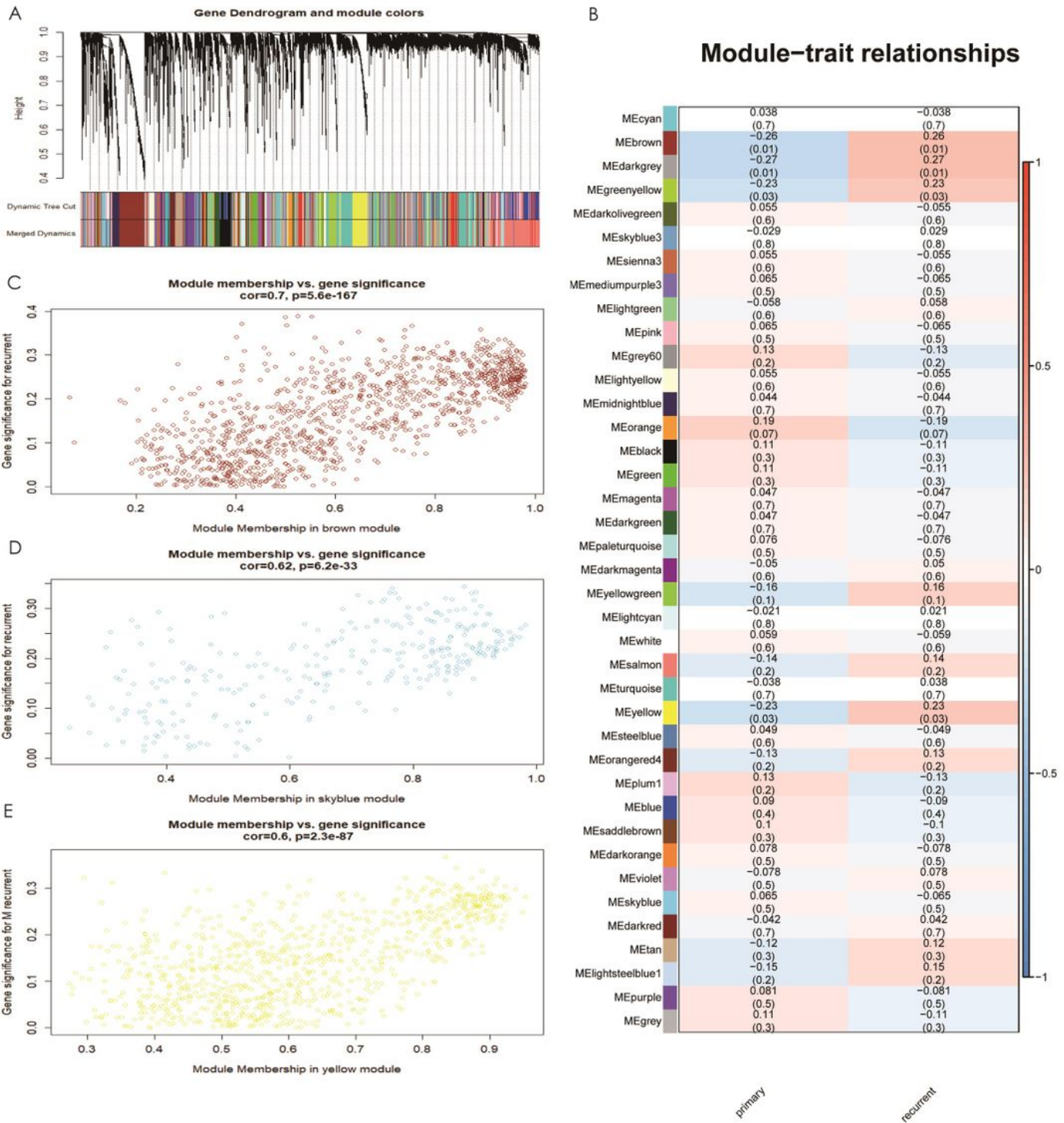


Figure 3

Relationship between clinic traits and significant modules identification. (A) A dendrograms of genes clustering before and after merging based on co-expression network analysis . a total of 52 co-expression modules were constructed and shown in different colors. (B) Association between module features. The brown, sky blue and yellow modules were the most relevant modules with recurrent traits. (C-E) Scatter plots of MM with module membership in brown, sky blue and yellow modules.

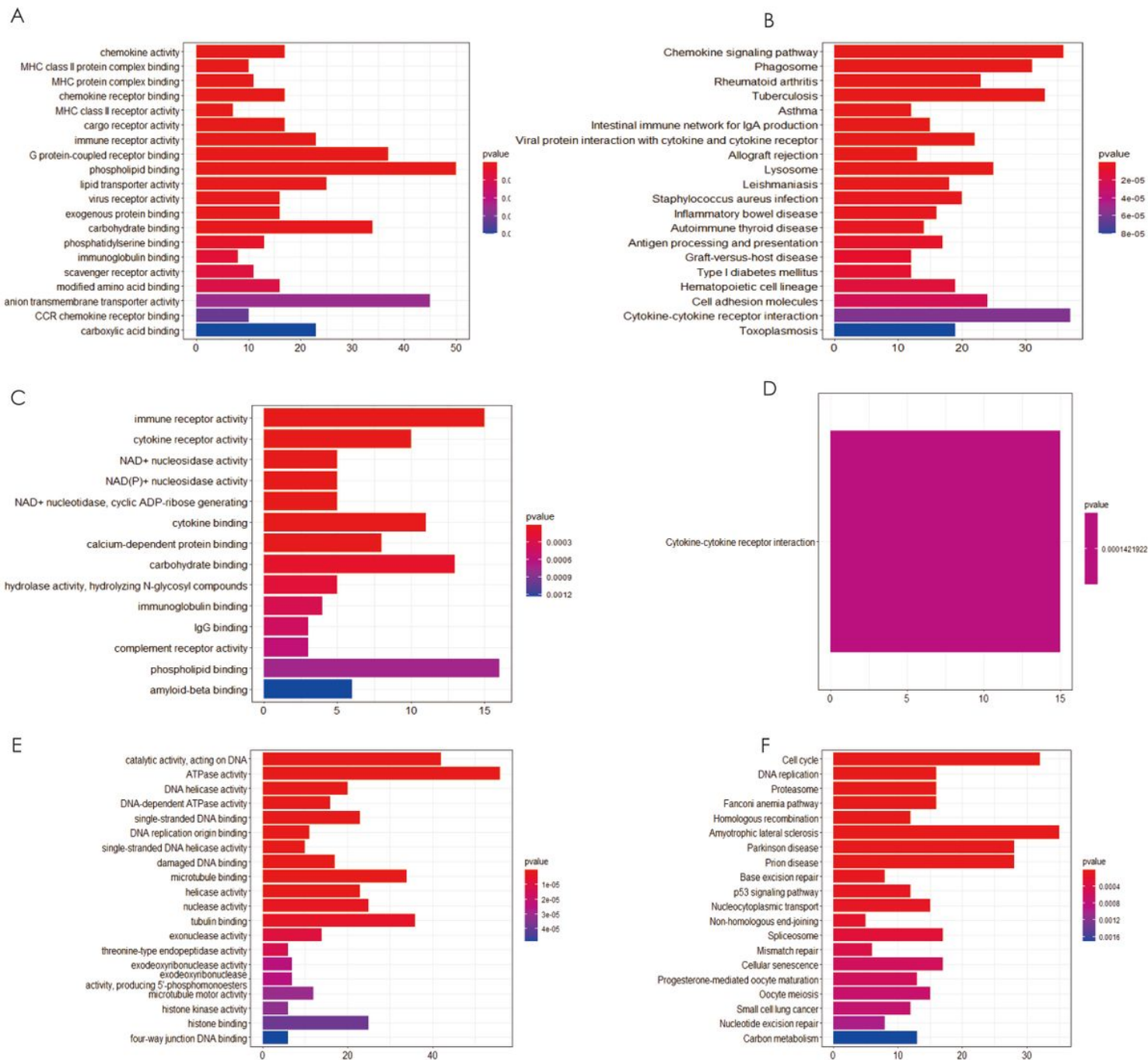


Figure 4

GO terms (A,C,E) and KEGG pathways enrichment analysis(B,D,F) of brown, sky blue and yellow module respectively.

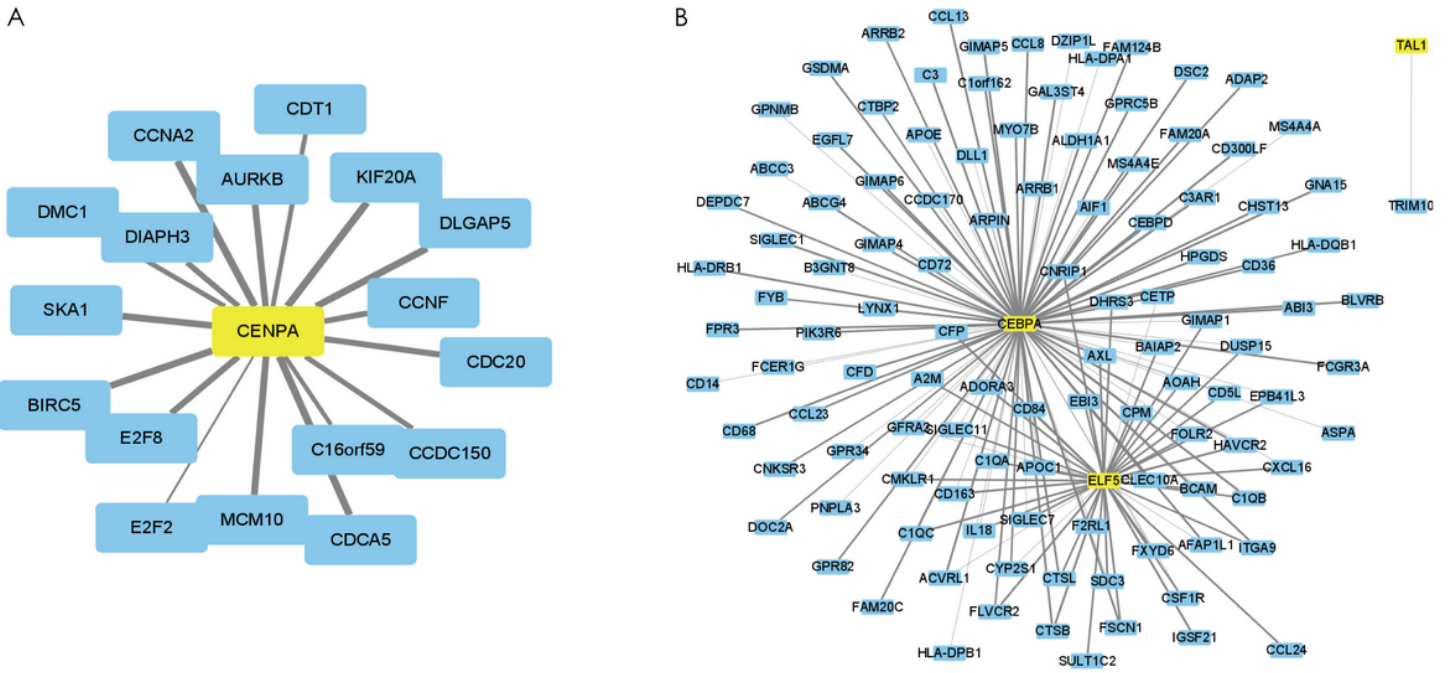


Figure 5

TATFs-gene regulatory network In yellow(A) and brown(B) modules.

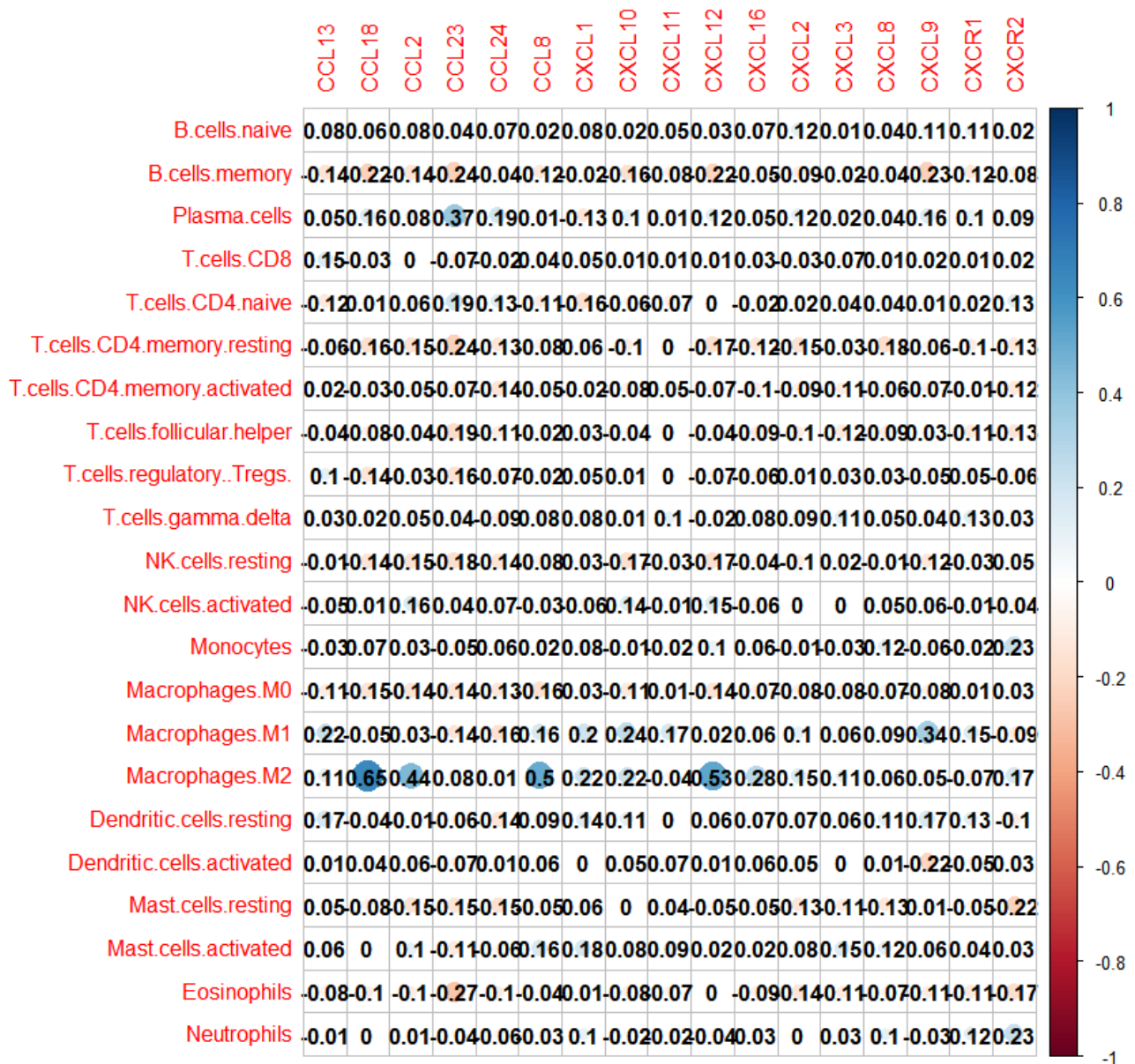


Figure 6

Gene expression of 17 different up-regulated cytokines and receptors in the brown and sky blue modules in relation to immune cell infiltration in the dataset GSE24080.

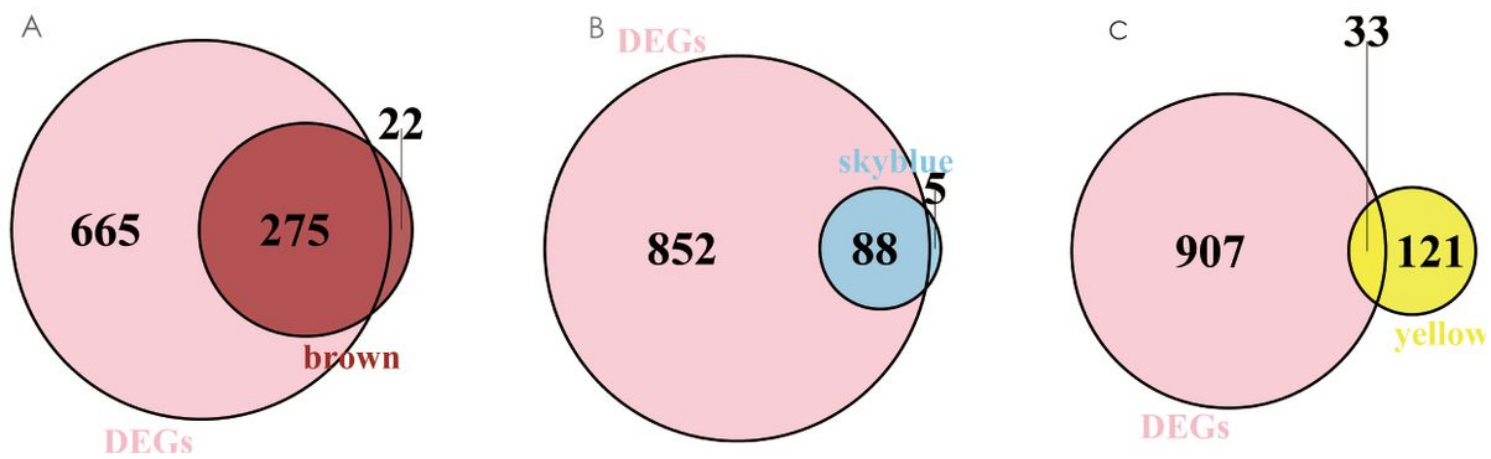


Figure 7

Venn diagram of DEGs and hub genes in each module

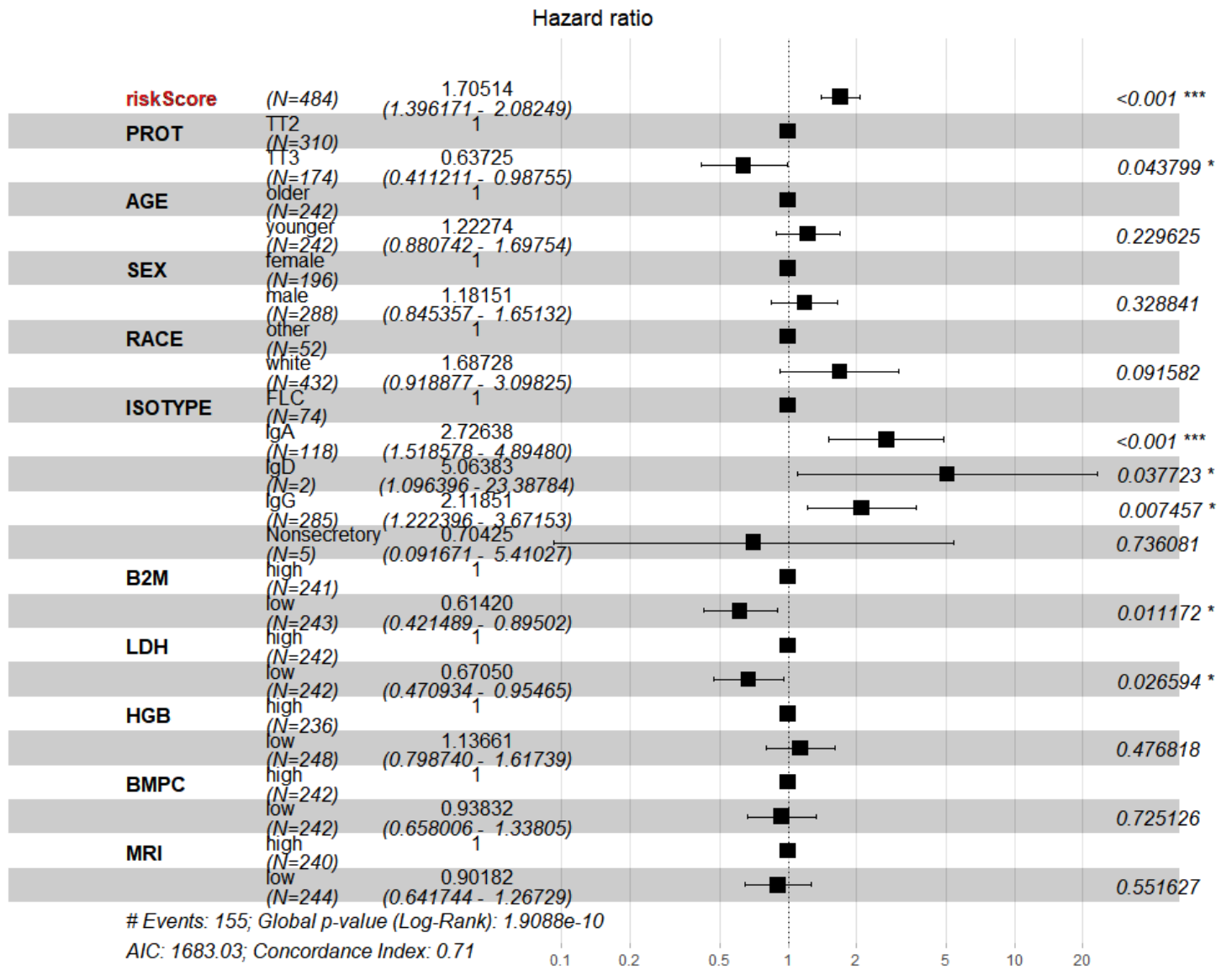


Figure 8

Multivariate association between the two-genes based on risk score prognostic model and clinical characteristics of EFS.

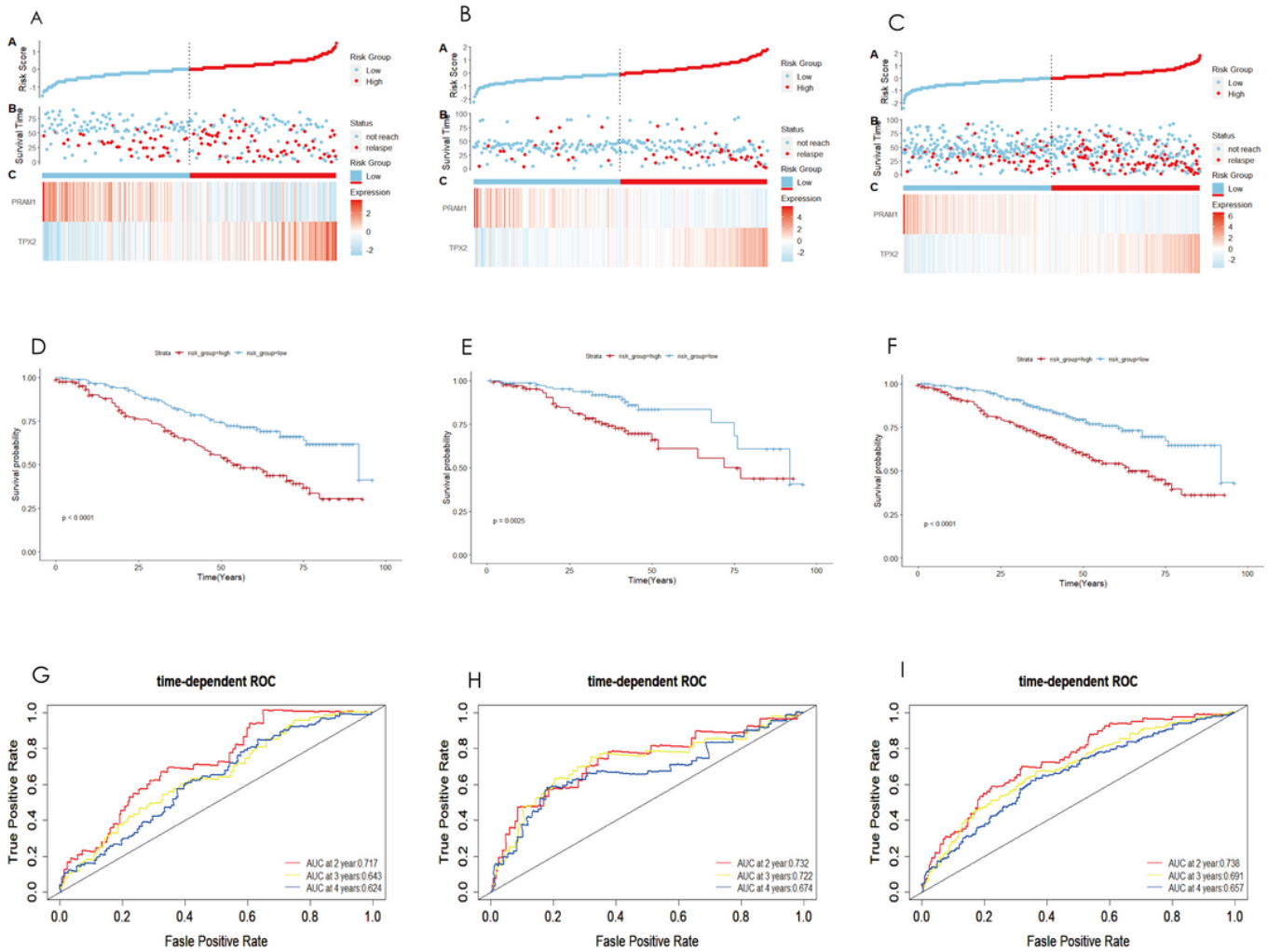


Figure 9

Construction and validation of prognostic risk model for MM patients. Risk score distribution and heat map of two prognostic genes(A–C) , and Kaplan-Meier curves in risk score (D-F) in the training set, validation set and overall set, respectively. (G–I) Time-dependent ROC curves for the prognostic model.

Supplementary Files

This is a list of supplementary files associated with this preprint. Click to download.

- [supplementaryfile.xlsx](#)